

# Simulation of tip-surface interactions in atomic force microscopy of an InP(110) surface with a Si tip

J. Tóbiš and I. Štich

*Department of Physics, Slovak Technical University (FEI STU), Ilkovičova 3, 812 19 Bratislava, Slovakia*

R. Pérez

*Departamento de Física Teórica de la Materia Condensada, Universidad Autónoma de Madrid, E-28049 Madrid, Spain*

K. Terakura

*JRCAT, National Institute for Advanced Interdisciplinary Research, 1-1-4 Higashi, Tsukuba, Ibaraki 305-8562, Japan  
and Institute of Industrial Science, University of Tokyo, Roppongi, Minato-ku, Tokyo 106-8558, Japan*

(Received 23 April 1999)

We present an *ab initio* simulation of short-range tip-surface interactions in the atomic force microscopy on the InP(110) surface with a neutral Si tip. Vertical scans over both types of surface atoms and a number of lateral scans (total energies and tip-surface forces) are calculated at the generalized gradient approximation level of the density-functional theory. Force calculation is used to estimate the frequency shift in real experiments in the frequency modulation mode. Analysis of the experimental results is performed on the basis of the simulation results. In particular, they provide an indication as to why only one (P) sublattice is experimentally observable with the Si tip. [S0163-1829(99)10039-0]

## I. INTRODUCTION

Atomic force microscopy<sup>1</sup> (AFM) is a surface-science method used to determine the atomic surface structure of both conductors and insulators. The main idea of this method is based on measuring the force between the sample surface and the tip. The atomic resolution could only be achieved in the non-contact operating mode in ultrahigh vacuum (UHV),<sup>2,3</sup> where the tip operates in an attractive regime. Since direct measurement of the force in this mode is not currently feasible, indirect methods for the measurement of tip-surface forces have been developed, such as the frequency modulation (FM) detection mode.<sup>4</sup> In the FM AFM the tip is mounted on a cantilever that oscillates with a known amplitude and frequency. As the tip comes to proximity of the surface, the tip-surface interaction causes a change of the oscillation frequency. In the usual operation mode, the frequency-shift mode, a scan at a constant frequency shift generates a topography of the atomic surface structure. By its nature AFM, probing the tip-surface interaction, is generally believed to be more directly related to the surface atomic structure than the scanning tunneling microscope (STM).

After the pioneering experiment by Giessibl,<sup>2</sup> which showed that atomic resolution with the FM AFM technique was feasible on the Si(111)-7×7 surface, more experiments have appeared on reactive semiconductor (110) surfaces such as InP(110),<sup>5,6</sup> GaAs(110), and InAs (110).<sup>7,8,9</sup> Recently, theoretical studies have started to shed light on the imaging mechanism of the FM AFM and on the delicate nature of the tip-surface interactions.<sup>10-12</sup> Both experiments<sup>13,14</sup> and theoretical investigations<sup>11,12,15</sup> revealed that the short-range chemical type of tip-surface interaction may be responsible for atomic resolution of the AFM. In this paper, we study the short-range (~5 Å) tip-surface interactions on the InP(110)

surface, which provide insights into the FM AFM experiments of Sugawara *et al.* on the same surface.<sup>5,6</sup> In addition, these results are also relevant for the experimental FM AFM results on related surfaces such as GaAs(110) (Ref. 7) and complementary to the theoretical study of the tip-surface interactions by Ke *et al.*<sup>16</sup> on the GaAs(110) surface. The experimental FM AFM images showed a lattice of elliptically shaped bright spots, which were interpreted as showing just one (anion) sublattice.<sup>5-7</sup>

For a number of reasons theoretical analysis of these results is rather complicated. These are as follows: (i) The nature of the tip-surface interaction is complicated as most studies<sup>11,12,15,7</sup> indicated that the atomic resolution in the FM AFM comes from the “chemical” interaction; (ii) Due to the large amplitude and low-tip oscillation frequency a direct atomistic simulation of the cantilever dynamics is *not* feasible in principle; (iii) The early ideas suggesting that the quantity probed by the FM AFM experiments was the force gradient of the tip-surface interaction were shown to be oversimplified.<sup>7</sup> One possible approach to the tip dynamics is the use of perturbation theory<sup>10</sup> as the tip oscillation amplitude is in the range of hundreds of angstroms whereas the ratio of the frequency shift to the basic oscillation frequency is of the order of 0.01%. All the different applications of the perturbation theory<sup>7</sup> reach basically the same conclusion giving support to (iii). We briefly touch on that point in Sec. III A where we apply the perturbation theory. This approach is complemented by lateral scans that give a quick qualitative insight into the experimental images.

Our main results are as follows: (1) Using the perturbation theory and our *ab initio* computed vertical scans we have determined the theoretical minimum tip-surface distance, which in turn could provide an estimate of the optimum operating mode;<sup>10</sup> (2) The computed AFM surface corrugation is in good agreement with experiments,<sup>5</sup> which

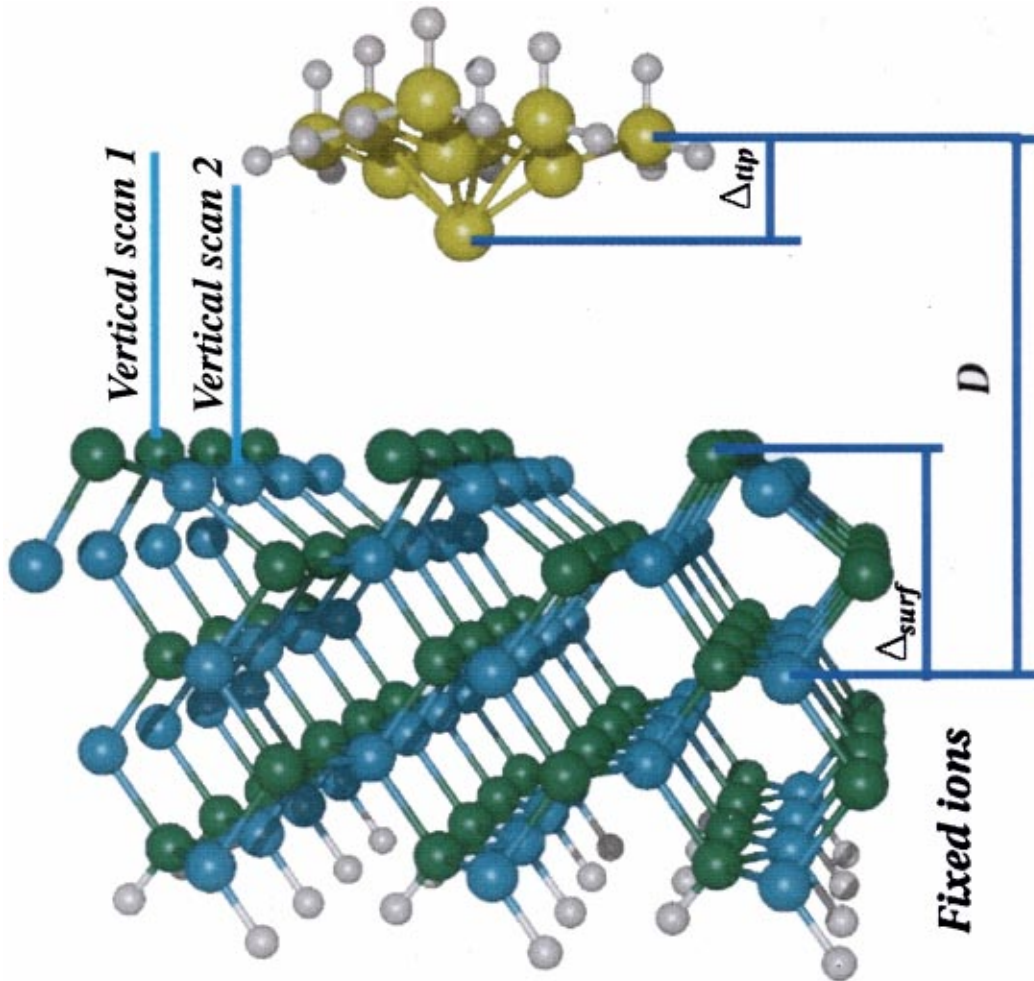


FIG. 1. (Color) Simulation geometry. The tip-surface distance is defined as  $d = D - \Delta_{tip} - \Delta_{surf}$  where  $\Delta_{tip}, \Delta_{surf}$  are taken before the mutual tip-surface interaction is switched on. The P atoms are the outermost atoms on the surface. The hydrogen termination is shown in white.

suggests that, despite all the simplifications, the basic ingredients in our approach are basically correct; (3) In agreement with experiments we conclude from the computed lateral scans that only one (P) sublattice should be experimentally detectable with a Si tip; (4) The results indicate that the spots in the experimental images need not necessarily coincide with the atomic positions.

The rest of the paper is organized as follows. The next section summarizes the technical details of our simulations. The results of our simulations are presented in Sec. III. Our main findings are summarized in Sec. IV.

## II. SIMULATION DETAILS

The most difficult part of the tip-surface interaction to model is the near contact short-range quantum-chemical part. This part is known to be well described<sup>11,12,17</sup> by the density-functional theory (DFT).<sup>18</sup> We have used the DFT in its plane-wave pseudopotential formulation.<sup>18</sup>

The InP(110) surface was modeled in a slab geometry using  $4 \times 3$  primitive surface unit cells. In direction perpendicular to the surface our slab consists of two free and three

fixed bulk-terminated layers (Fig. 1). The unit cell size in this direction was set to 23.0 Å. With this value the minimum distance between the top layer of the tip and the bottom layer of the surface (caused by periodic conditions) was  $\approx 4$  Å. This value was found sufficient. There are 60 In and 60 P atoms in the slab and 24 H atoms are used to terminate the bottom of the slab. A similar slab thickness was used by Alves *et al.* in the study of clean III-V surfaces.<sup>19</sup> Si tips have been used in the experiments<sup>5,6</sup> and hence we modeled the tip by 10 Si atoms arranged in (111) planes and 15 H atoms were used to terminate the free-dangling bonds in the tip base (c.f. Fig. 1). The idea is to saturate the dangling bonds in the tip base while leaving one dangling bond sticking out of the tip apex. The apex and its three nearest-neighbor Si atoms of the tip are allowed to move, while the remaining atoms are fixed to emulate the bulk-tip termination. The free atoms were allowed to move in direction of the force, until the forces became negligible small. The sum of the forces exerted on the fixed atoms of the tip is taken to be the total tip-surface force. The properties of this tip have been extensively studied in Refs. 11 and 12 and it was shown that the results are relatively insensitive to the tip size.

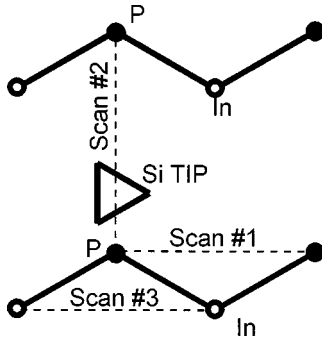


FIG. 2. Schematics of the lateral scans performed. The tip orientation is shown by the triangle over the P atom.

The total energy and forces were calculated within DFT in the generalized gradient approximation (GGA).<sup>20</sup> The implementation of the GGA functional followed Ref. 21. The energy cutoff was set to  $E_{\text{cut}}=8$  Ryd. This value was found to produce converged structures for the clean InP(110) surface.<sup>19</sup> In particular, our computed value of the surface buckling  $\Delta_{1\perp}=0.645$  Å is in perfect agreement with that of Ref. 19. Optimized nonlocal pseudopotentials<sup>22,23</sup> were used for all elements except for H, which was described by bare Coulomb potential. Brillouin zone was sampled at the  $\Gamma$  point. The effect of this sampling on the resulting tip-surface interaction for reactive surfaces with similarly sized unit cells was in detail studied in Ref. 12. The total energy was calculated using the conjugate gradients techniques<sup>24</sup> with the accuracy of  $1 \times 10^{-4}$  eV; the threshold for the ionic force convergence was set to  $2 \times 10^{-2}$  eV/Å  $\approx 3.2 \times 10^{-2}$  nN.

We have performed simulations of the operation of the AFM apparatus by making stepwise small static movements of the tip in both horizontal and vertical directions. As the tip oscillation frequencies are many orders of magnitude lower than frequencies typical for the atomic motion we expect that these simulations provide an accurate description of the imaging process. In this manner we performed calculations of both vertical (over the P and In atoms) and horizontal scans, henceforth called displacement curves and lateral scans, respectively. The tip orientations along with the directions of the lateral scans are shown in Fig. 2. There is a difficulty to determine the tip-surface distance, since both the tip and the surface undergo pronounced relaxations as the tip comes to close proximity of the surface. Hence, the tip-surface distance is defined by the distance of the fixed layers subtracted from the thickness of the free layers before the mutual tip-surface interaction is switched on (c.f. Fig. 1). This definition is also useful for determination of the frequency shift by the perturbation theory. The atomic relaxations leading to the differences between the “tip-surface” and “apex-surface atom” distances have been discussed in Ref. 12.

### III. SIMULATION RESULTS

The FM AFM experiments could be analyzed by simulating the vertical tip oscillation, which in turn would require the knowledge of the displacement curves over the whole area of the surface unit cell. The tip motion could be described either in a perturbation approach or by directly simulating the tip oscillation. In either case the problem with this approach is that in order to generate a computed image,

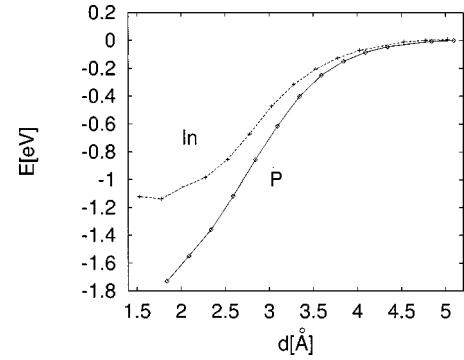


FIG. 3. Short-range part of the interaction energy over both types of the surface atoms as a function of the tip-surface distance (vertical scan #1 and #2 of Fig. 1). The lines are guides to the eye.

which could be compared to the experimental AFM image or just to map out an AFM image of an atom would require an inordinate number of calculations and analyses, which is currently not feasible in an *ab initio* manner. Because of this limitation we follow the perturbation theory approach in Sec. III A just for the tip positions on top of the P and In atoms. In order to get a quick qualitative insight into the experimental images we have performed a number of lateral scans to be discussed in Sec. III B.

#### A. Displacement curves

The calculated displacement curves over the P and In atoms are shown in Figs. 3 and 4. Similarly to our previous experience with the Si(111)- $5 \times 5$  surface<sup>12</sup> these results show pronounced deviations from functional dependences designed to describe simple bonding situations such as the Morse or Rydberg function. However, these results deviate appreciably also from the theoretical results for the Si(111)- $5 \times 5$  surface.<sup>12</sup> This is likely a consequence of the  $1 \times 1$  periodicity on the InP(110) surface where the surface atoms are closer to each other compared to the adatoms on the Si(111) surface. This situation favors multibond interactions between the tip and the surface on the InP(110) surface. At short distance, we observe over both ions a very signifi-

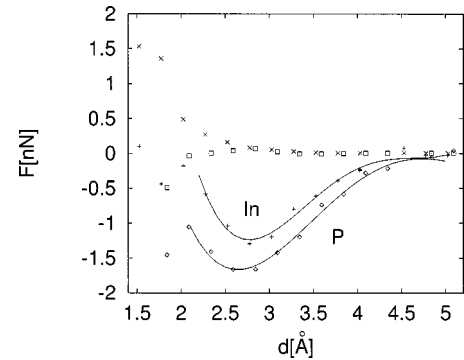


FIG. 4. Short-range part of the normal (diamonds, pluses) and lateral (crosses, squares) tip-surface force over both types of the surface atoms as a function of the tip-surface distance (vertical scan #1 and #2 of Fig. 1). Note the large lateral force acting on the tip at the In site (crosses) and to a lesser extent also over the P site (squares). This lateral force modifies the tip structure. The lines for  $d > 2$  Å are polynomial fits to the computed normal forces.

cant surface response leading to a complicated medium range tip-induced surface relaxation. Surprisingly, the minima of the force curves over both atoms are very close to each other despite the surface buckling of the clean surface being  $0.645 \text{ \AA}$ . This occurs because the P atom relaxes downwards in response to the tip whereas the In atom does not. In addition, over the In atom around  $d \approx 2 \text{ \AA}$  we observe an onset of a large lateral force on the tip apex, which significantly modifies the tip structure. Basically, around that distance the tip dangling bond starts forming a bond to one of the nearby P atoms. This force is clearly reflected in the energy and force curves. It is interesting to compare this behavior to that of the Ga atom on the GaAs(110) surface where, in addition to similar tip structure modification, a jump of the Ga atom towards the tip with a complicated hysteretic behavior occurs.<sup>16</sup> Moreover, in marked difference to InP, the force curve over the As atom exhibits multiple minima.<sup>16</sup> Hence, the GaAs(110) surface in the direction perpendicular to the surface appears “softer” to the Si tip than the InP(110) surface.

The calculated displacement curves can be analyzed using the perturbation theory. As mentioned above, the tip-surface interaction can be considered a small perturbation to the harmonic oscillations of the tip.<sup>10</sup> In the simplest case the Hamiltonian of the tip reads

$$H = \frac{p^2}{2m} + \frac{kq^2}{2} + V_p(q) = E, \quad (1)$$

where  $V_p(q)$  is the perturbation potential,  $k$  the tip-spring constant and the frequency of the unperturbed oscillator is  $\nu_0 = 1/2\pi\sqrt{k/m}$ . The energy term  $E$  on the right-hand side of Eq. (1) indicates that the Hamiltonian is time independent—i.e., energy conserved. This approach neglects the tip damping (infinite quality factor  $Q$  of the cantilever/tip) as well as the possible perturbation of the oscillation amplitude.

Using standard methods of canonical transformations<sup>25</sup> this Hamiltonian can be transformed to action-angle variables

$$H = J_0\nu_0 + V_p(J_0, w_0) \\ w_0 = \nu_0 t + \beta \quad J_0 = 1/\nu_0 E_0. \quad (2)$$

The result is that for an unperturbed system, the Hamiltonian is expressed only in terms of the canonical momentum. The perturbation theory searches for new canonical coordinates, in which the entire Hamiltonian is again expressed only by the canonical momentum.<sup>10,25</sup> This procedure leads to the following expression for the perturbed frequency

$$\nu = \nu_0 + \frac{\partial \bar{V}_p}{\partial J_0}. \quad (3)$$

Here,  $\bar{V}_p$  is the averaged value of the perturbation over the whole path of the tip during one period. From this equation it follows that the frequency shift is *not* proportional to the tip-surface force gradient.<sup>26</sup>

We have fitted the vertical part of the computed force displacement curves (c.f. Fig. 4). Integrating these functions we have obtained the perturbation potential  $V_p(d)$  for the vertical motion of the tip.<sup>27</sup> According to Eq. (1) this poten-

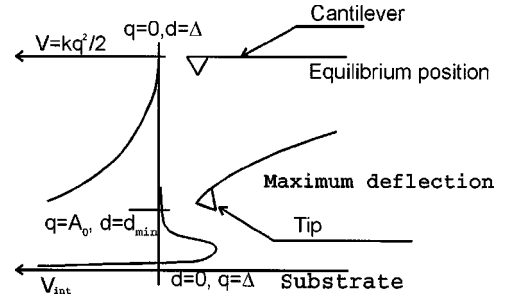


FIG. 5. Schematics of the FM AFM experiment. The spring and the tip-surface potential are shown on the left. The relation between  $q$ ,  $d$ , and  $\Delta$  is given by  $d + q = \Delta$ .  $\Delta$  is changing so slowly, that it can be considered to be constant during one period.

tial must be expressed in the  $q$  coordinate system. This transformation depends on  $\Delta$ , the distance between the substrate surface and the tip equilibrium position (Fig. 5). Therefore  $V_p(q)$  in Eq. (1) is given by  $V_p(q) = V_{\text{int}}(\Delta - q)$ . The frequency shift was then determined as a function of  $d_{\text{min}}$  defined as the shortest distance between the tip and the surface during the whole trajectory of the tip. The other parameters that enter the calculation were taken from the experiment.<sup>5</sup> The calculated frequency shift and the parameters used are in Fig. 6. Considering that  $\Delta f$  was set to  $-6 \text{ Hz}$  in the experiment, we find that  $d_{\text{min}}$  is  $\sim 3.3$  and  $\sim 3.0 \text{ \AA}$  over the P and In atom, respectively. From these numbers we estimate a surface corrugation of  $\approx 0.3 \text{ \AA}$ . This value is in a good agreement with the value of the corrugation of  $0.19 \pm 0.05$  and  $0.12 \text{ \AA}$  for  $[001]$  and  $[1\bar{1}0]$  direction, respectively.<sup>5</sup> The latter value is more relevant. Such a good agreement is surprising for a number of reasons. Firstly, our modeling does *not* take into account the long-range van der Waals interactions. Secondly, we consider an ideal tip with a single unsaturated dangling bond, whereas the tip-surface interaction in a real experiment is likely to be more involved. This indicates that the experiments must have been performed with a very sharp tip. It is also interesting to observe that a measurable frequency shift of  $-6 \text{ Hz}$  is generated over a very short-range distance of  $\sim 2 \text{ \AA}$  in the perturbation potential (i.e. for  $3 \text{ \AA} < d < 5 \text{ \AA}$ ).

## B. Lateral scans

Using the estimates for the minimum tip-surface distance from Sec. III A we have chosen to sample the lateral scans at

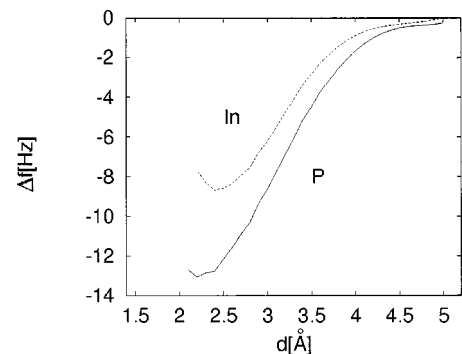


FIG. 6. Frequency shift as a function of the tip-surface distance  $d$ . In calculation of these functions we have used the experimental parameters (Ref. 5) ( $\nu_0 = 151 \text{ kHz}$ ,  $k = 34 \text{ N/m}$ ,  $A_0 = 200 \text{ \AA}$ , and  $\Delta f = -6 \text{ Hz}$ ).

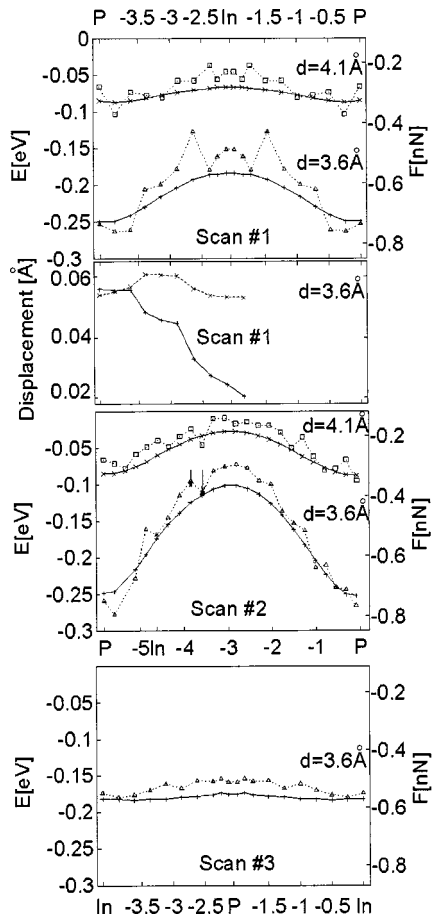


FIG. 7. Short-range interaction energy (full lines) and normal tip-surface force (dotted lines) for the lateral scans (c.f. Fig. 2) with the tip scanning at the tip-surface distance  $d$  indicated in the panels. Positions of the atoms on the scan axis as well as the positions of the nearby off-axis atoms are also shown. For scan #1 we show in the second panel from the top the total displacements (in Å) of two surface In atoms showing discontinuities in their relaxation pattern. In the scan #2 the arrows indicate the two points recalculated by bringing pristine tip and surface to the distance of 3.6 Å.

two different tip-surface distances: 4.1 and 3.6 Å. In the short-range regime investigated here these distances are typical for very weak and stronger “chemical” type of tip-surface interaction. In order to cover the most important sections of the surface we have performed two scans along the In-P chain (scans #1 and #3 in Fig. 2) and one in direction perpendicular to the chain (scan #2 in Fig. 2).

The results for scan #1 are shown in Fig. 7. Clearly the scan taken at the smaller tip-surface distance is more corrugated. We note that the minima of both energy and force curves are positioned close to the phosphorus atoms but do not necessarily coincide with the positions of the P atoms. An interesting feature of the force curves are their “spiky” shapes. As shown in the lower panel of Fig. 7 this feature can be traced back to discontinuities in the lateral relaxation of some surface atoms. We attribute them to the shape of the high-dimensional potential energy surface, which causes some of the surface atoms move discontinuously over the energy barriers separating two minima as we move the tip base. Note that in energy terms these features are extremely tiny and would be washed out at finite temperatures. We

have checked that these spikes are genuine features of the force curves. All lateral scans were computed by making small lateral displacements to the tip taking the initial tip and surface atomic structures from the previous step and performing a complete electronic/ionic relaxation. In scan #2 we have recalculated two points (c.f. Fig. 7) by bringing a pristine surface and tip to the required tip-surface distance. As can be seen the results of the two calculations coincide to within the threshold of our force optimization, corroborating the genuine character of the force curves. In the scan #2, the minima of the curves are again close to the P atoms albeit not necessarily coinciding with the atomic positions. Moreover, there is an asymmetry in the curves, which we attribute to the polar covalent character of the In-P bond causing the centroid of the bond charge to be displaced towards but not coincide with the position of the P atom. The fact that most of the reactive charge responsible for the minima in the lateral scans floats on the P atoms is reflected in the results of scan #3 shown in Fig. 7. Since most of the reactive charge is located away from the In atoms, the tip does not “see” any corrugation in the scan direction #3 despite the magnitude of both the energies and forces being comparable to that in the other scan directions. From this we conclude that, given the charge distribution, it would be difficult to significantly enhance the resolution of the In atoms even if the tip could come closer to the In atom.

#### IV. SUMMARY AND CONCLUSIONS

We have used *ab initio* total energy techniques to investigate the short-ranged chemical type of tip surface interactions in the non-contact AFM for InP(110) surface probed by a silicon tip. Our calculations give an insight into why only the anion lattice is experimentally observed on the III-V surfaces. Comparison of these results with those for the GaAs surface<sup>16</sup> reveals a number of striking differences. Most of them are manifestation of the fact that the Si tip sees much a “softer” potential energy surface over the GaAs surface than over the InP surface. However, most of these differences may not appear in the FM AFM images as the experiments operate further away from the surface. Our results also indicate that, due to the chemical nature of the tip-surface interactions, the spots in the experimental images may not coincide with the positions of the atoms. This may be important if adsorbates or defects are imaged. These conclusions have been reached from very simple modeling with a very sharp tip and excluding the van der Waals interactions. The fact that the AFM surface corrugation computed in the perturbation theory is in a reasonable agreement with the experimental value strongly suggests that the experiments have been done with very sharp tips and that it is indeed the chemical type of interaction responsible for the atomic resolution. Using identical model for the tip-surface interaction on the Si(111)-5×5 surface<sup>11,12</sup> a similar semiquantitative agreement with the experiments<sup>2</sup> has been achieved. However, the complexity of this interaction further complicated by deformation of both the tip and the surface during the imaging process suggests that, contrary to the naive expectation, interpretation of the experimental AFM images may be of comparable complexity to that of STM.

## ACKNOWLEDGMENTS

The calculations were performed on the JRCAT super-computer system. This work was partly supported by the New Energy and Industrial Technology Development Orga-

nization (NE-DO). I.S. thanks JRCAT and the Atom Technology Partnership for support. R.P. acknowledges financial support from the CICyT (Spain) under Contract No. PB97-0028.

- <sup>1</sup>G. Binnig, C. F. Quate, and Ch. Gerber, *Phys. Rev. Lett.* **56**, 930 (1986).
- <sup>2</sup>F. J. Giessibl, *Science* **267**, 68 (1995).
- <sup>3</sup>S. Kitamura and M. Iwatsuki, *Jpn. J. Appl. Phys., Part 2* **35**, L145 (1995).
- <sup>4</sup>T. R. Albrecht, P. Grütter, D. Horne, and D. Rugar, *J. Appl. Phys.* **69**, 668 (1991).
- <sup>5</sup>Y. Sugawara, M. Ohta, H. Ueyama, and S. Morita, *Science* **270**, 1646 (1995).
- <sup>6</sup>H. Ueyama, M. Ohta, Y. Sugawara, and S. Morita, *Jpn. J. Appl. Phys., Part 1* **34**, 1086 (1995).
- <sup>7</sup>See, for instance, *Proceedings of the First International Workshop on Noncontact AFM* [*Appl. Surf. Sci.* **140** (3, 4) (1999)].
- <sup>8</sup>A. Schwarz, W. Allers, U. D. Schwarz, and R. Wiesendanger, *Appl. Surf. Sci.* **140**, 293 (1999).
- <sup>9</sup>M. Ohta, Y. Sugawara, F. Osaka, S. Ohkouchi, M. Suzuki, S. Mishima, T. Okada, and S. Morita, *J. Vac. Sci. Technol. B* **13**, 265 (1995).
- <sup>10</sup>F. J. Giessibl, *Phys. Rev. B* **56**, 16 010 (1997).
- <sup>11</sup>R. Pérez, M. C. Payne, I. Štich, and K. Terakura, *Phys. Rev. Lett.* **78**, 678 (1997).
- <sup>12</sup>R. Pérez, I. Štich, M. C. Payne, and K. Terakura, *Phys. Rev. B* **58**, 10 835 (1998).
- <sup>13</sup>T. Uchihashi, Y. Sugawara, T. Tsukamoto, M. Ohta, S. Morita, and M. Suzuki, *Phys. Rev. B* **56**, 9834 (1997).
- <sup>14</sup>R. Erlandsson, L. Olsson, and P. Martenson, *Phys. Rev. B* **54**, R8309 (1996).
- <sup>15</sup>N. Sasaki and M. Tsukada, *Jpn. J. Appl. Phys., Part 1* **38**, 192 (1999).
- <sup>16</sup>S. H. Ke, T. Uda, R. Pérez, I. Štich, and K. Terakura, preceding paper, *Phys. Rev. B* **60**, 11631 (1999).
- <sup>17</sup>See, for instance, S. Ciraci, E. Tekman, A. Baratoff, and I. P. Batra, *Phys. Rev. B* **46**, 10 411 (1992); S. Ciraci, A. Baratoff, and I. P. Batra, *ibid.* **41**, 2763 (1990).
- <sup>18</sup>See, for instance, M. C. Payne, M. P. Teter, D. C. Allan, T. A. Arias, and J. D. Joannopoulos, *Rev. Mod. Phys.* **64**, 1045 (1992).
- <sup>19</sup>J. L. Alves, J. Hebenstreit, and M. Scheffler, *Phys. Rev. B* **44**, 6188 (1991).
- <sup>20</sup>We use the Perdew-Wang 91 functional, see, for instance, J. P. Perdew, *et al.*, *Phys. Rev. B* **46**, 6671 (1992).
- <sup>21</sup>J. A. White and D. Bird, *Phys. Rev. B* **50**, 4954 (1994).
- <sup>22</sup>A. Rappe, K. M. Rabe, E. Kaxiras, and J. D. Joannopoulos, *Phys. Rev. B* **41**, 1227 (1990).
- <sup>23</sup>J. S. Lin, A. Qteish, M. C. Payne, and V. Heine, *Phys. Rev. B* **47**, 4174 (1993).
- <sup>24</sup>We use an all-band conjugate gradient optimization of the electronic structure closely related to the algorithms described in I. Štich, R. Car, M. Parrinello, and S. Baroni, *Phys. Rev. B* **39**, 4997 (1989); and M. J. Gillan, *J. Phys.: Condens. Matter* **1**, 689 (1989). In addition, the algorithm for electronic degrees of freedom is combined with a conjugate gradient optimization of the ionic degrees of freedom.
- <sup>25</sup>See, for instance, W. Dittrich, and M. Reuter, *Classical and Quantum Dynamics* (Springer, Berlin, 1996), pp. 75–117.
- <sup>26</sup>For example, for a polynomial perturbation potential  $V_{\text{int}} = cq^n$  one obtains  $\Delta f = ncA_0^{n-2}f_0/k\langle \sin^n \rangle$ , which is not the force gradient because this function does not have the proper dependence on  $n$ .
- <sup>27</sup>The perturbation potential beyond the tip-surface distance of 5.1 Å is taken to be zero.